$ZnIn_2S_4$ nanosheets with tunable dual vacancies for efficient sacrificial-agent-free H_2O_2 photosynthesis

Chen Zhang, ‡[a,d] Gao Xu, ‡[a] Qifeng Liang, [a] Li Liang, [a] Zebo Fang, [a] Rong Wu, [d] Shunhang Wei, [a,*] Lei Wang, [c,*] Xiaoxiang Xu, [b,*]

[a] *Zhejiang Engineering Research Center of MEMS, Shaoxing University, Shaoxing 312000, China*

[b] *School of Chemical Science and Engineering, Tongji University, Shanghai, 200092, China*

[c] *School of Environmental Science and Engineering, Guangzhou University, Guangzhou, 510006, China*

[d] *School of Physics Science and Technology, Xinjiang University, Urumqi 830000, China*

‡ These authors contribute equally

*Corresponding authors. E-mail addresses: wsh@usx.edu.cn (S. Wei); lwang866@163.com (L. Wang); xxxu@tongji.edu.cn (X. Xu).

Characterization

An X-ray powder diffractometer (XRD, Empyrean) and a Raman spectrometer (LabRAM HR Evolution) were used to detect the crystal structure of the obtained samples. A field emission scanning electron microscope (FESEM, SIGMA 300) and a high-resolution transmission electron microscope (HRTEM, JEM-2100F) equipped with an energy dispersive X-ray spectrometer (EDS) were used to observe their morphology and elemental distributions. The time-resolved PL (TRPL) decay spectra were recorded using a spectrofluorometer (FLUOROLOG-3-11) with an excitation wavelength of 370 nm (detection wavelength was 512 nm). The surface states of the samples were characterized by an X-ray photoelectron spectroscopy (XPS, Thermo Scientific K-Alpha+), and the binding energies calibrated to the C 1s peak at 284.8 eV. The UV-vis diffuse reflection spectra (DRS) of the samples were collected on an UV-vis spectrophotometer (Shimadzu UV-3600 plus) equipped with an integrating sphere assembly, and $BaSO_4$ was used as the non-absorbing reference material. Electron paramagnetic resonance (EPR) spectra were recorded on a Bruker EMXPLUS at room temperature. The composition of samples was explored using inductively coupled plasma optical emission spectrometry (ICP-OES, Optima 8300) and organic element analyzer (OEA, Elemantar: Vario EL cube). The steady-state surface photovoltage (SPV) spectra were collected in a CEL-SPS1000 spectroscopic analysis system containing a 500 W Xenon lamp (CEL-S500).

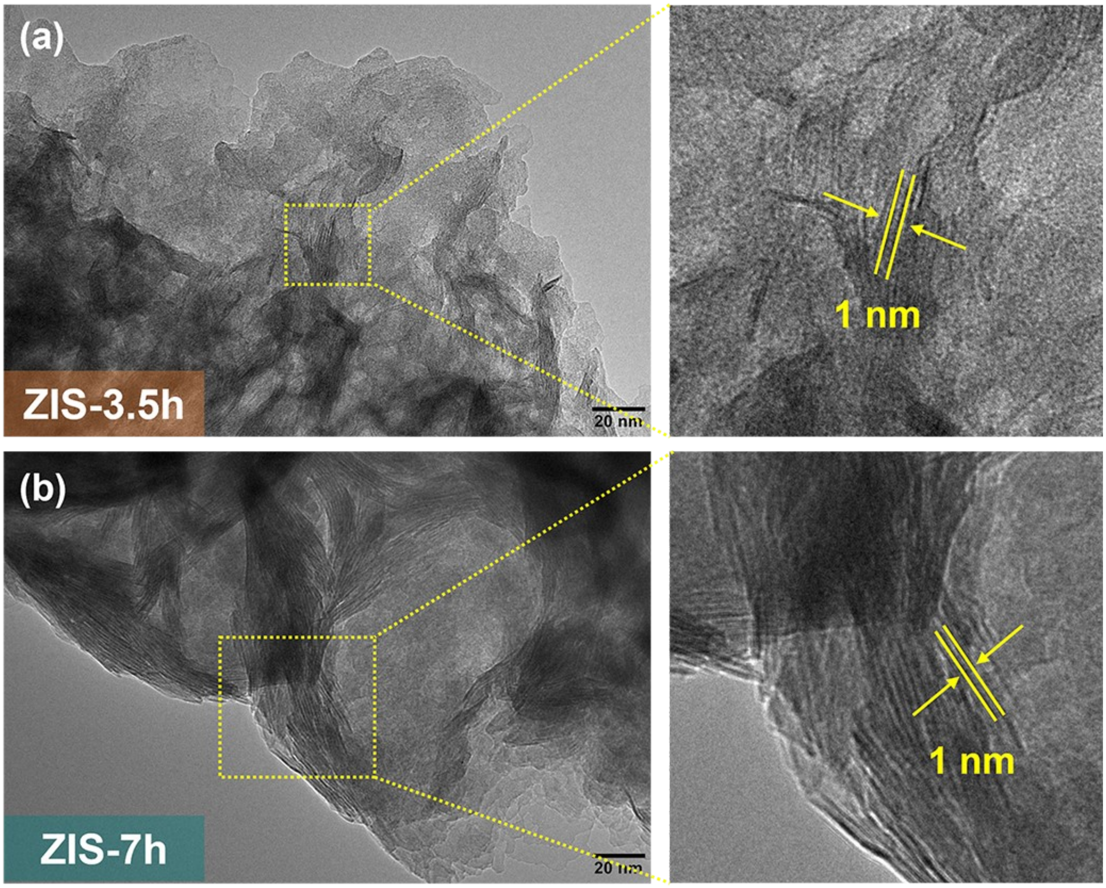

Fig. S1 TEM images of (a) ZIS-3.5h and (b) ZIS-7h.

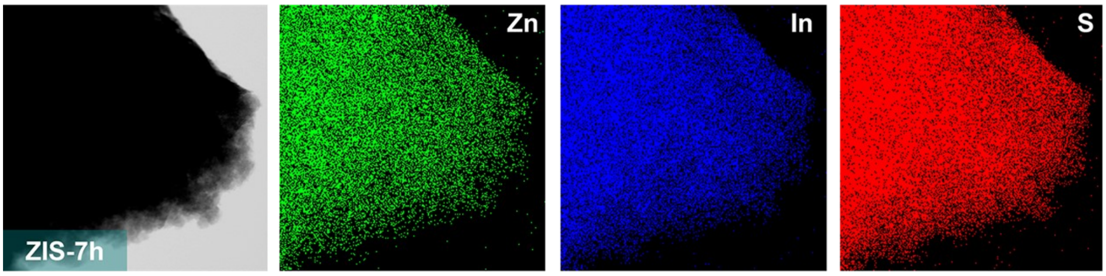

Fig. S2 the corresponding elemental mapping of the ZIS-7.

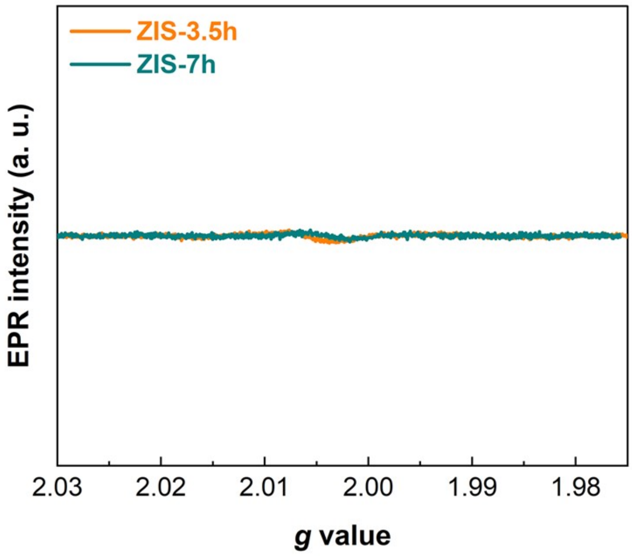

Fig. S3 EPR spectra of the ZIS-3.5h and ZIS-7h samples.

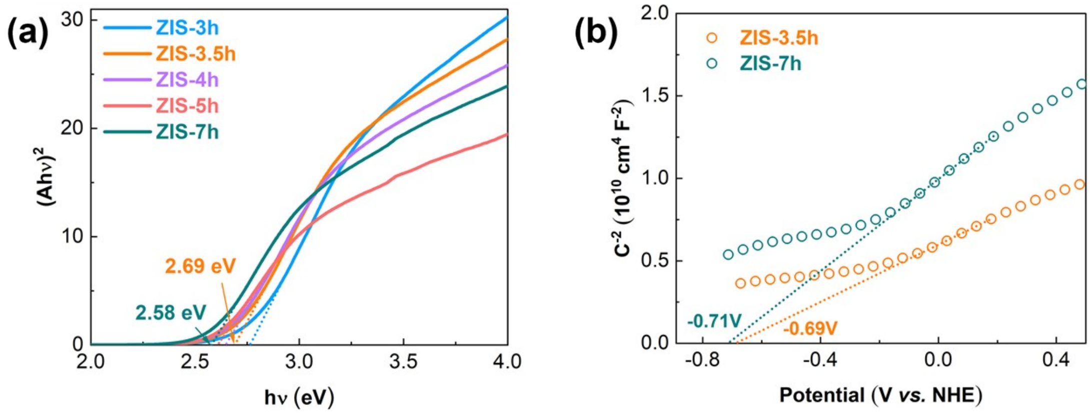

Fig. S4 (a) the Tauc plot and (b) Mott-Schottky plots of the as-prepared samples.

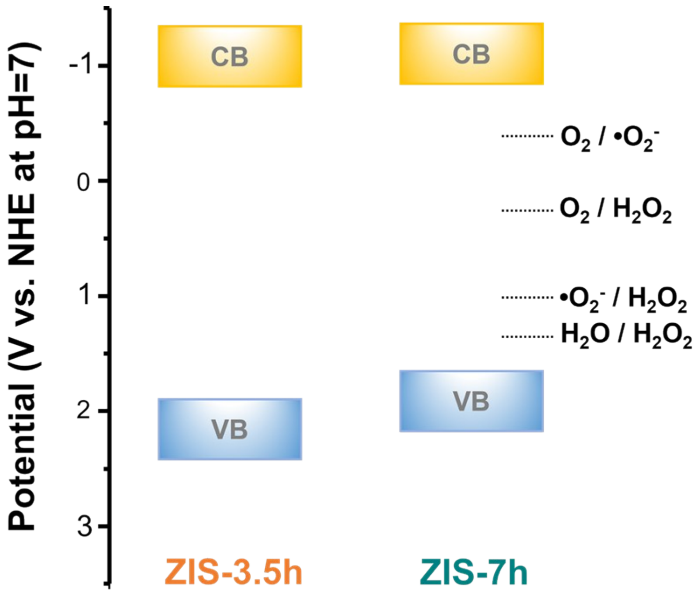

Fig. S5 Schematic illustration of band structure of the as-prepared samples.

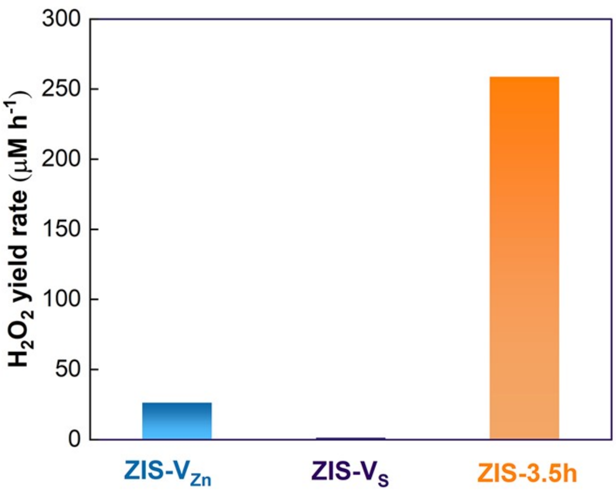

Fig. S6 Photocatalytic H_2O_2 yield rate of different samples in O_2 - saturated pure water under AM1.5 irradiation.

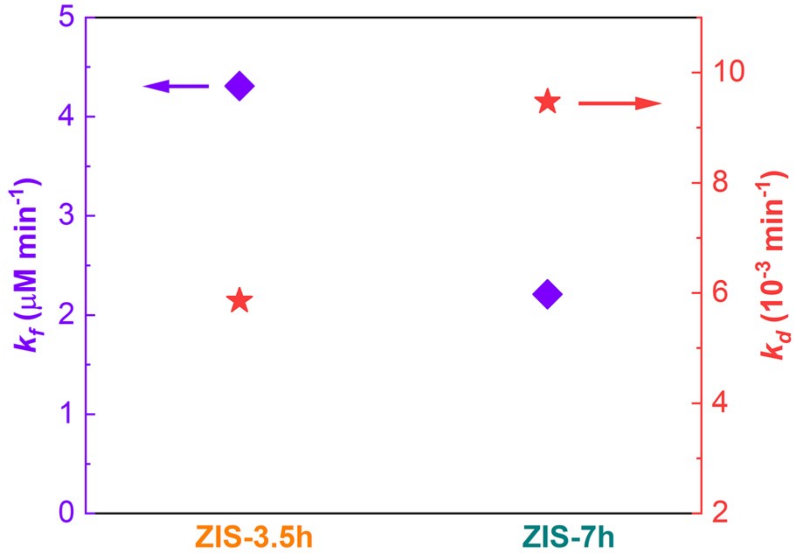

Fig. S7 K_f and K_d constant of the ZIS-3.5h and ZIS-7h.

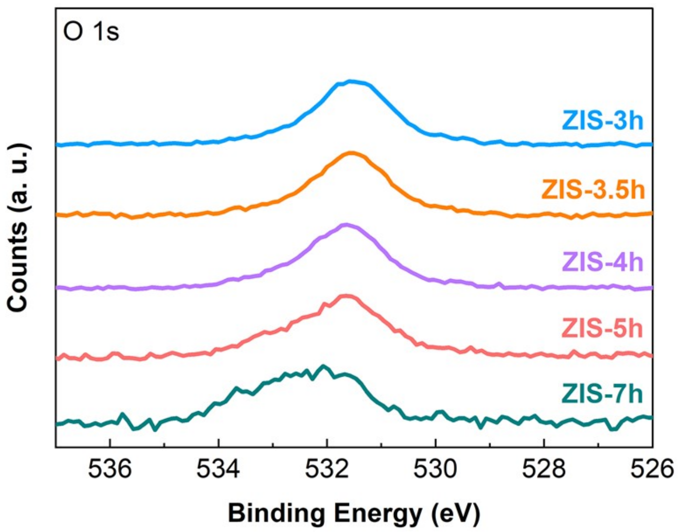

Fig. S8 The O 1s peaks of the as-prepared samples.

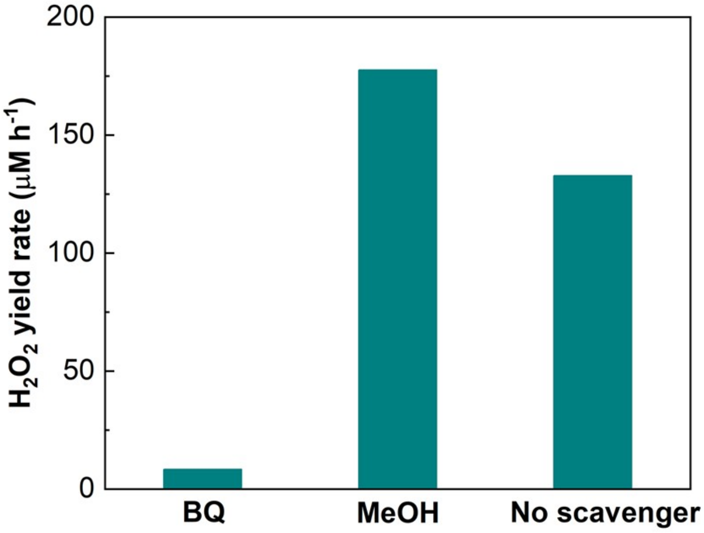

Fig. S9 Active species capture experiments over ZIS-7h under AM1.5 irradiation.

Table S1. The element atom contents measured by XPS.

Samples	Zn (at.%)	In (at.%)	S (at.%)	O (at.%)	C (at.%)	Zn : In : S : O atom ratio
ZIS-3h	5.11	21.14	23.10	23.75	26.90	0.48 : 2 : 2.18 : 2.25
ZIS-3.5h	8.66	20.93	25.87	20.61	23.93	0.82 : 2 : 2.47 : 1.97
ZIS-4h	10.83	19.18	27.04	16.97	25.35	1.13 : 2 : 2.82 : 1.77
ZIS-5h	16.18	18.50	30.27	11.55	23.49	1.75 : 2 : 3.27 : 1.25
ZIS-7h	17.00	15.15	27.59	9.88	30.38	2.24 : 2 : 3.64 : 1.30

Table S2. The element atom contents measured by EDS

Samples	Zn (at.%)	In (at.%)	S (at.%)	Zn : In : S atom ratio
ZIS-3.5h	6.89	41.16	51.59	0.33 : 2 : 2.51
ZIS-7h	13.15	29.77	57.08	0.88 : 2 : 3.83

Table S3. The inductively coupled plasma optical emission spectroscopy (ICP-OES) data of ZIS-3.5h.

Samples	Test elements	Sample element content W (%)	ICP normalization
ZIS-3.5h	Zn	5.41	$Zn_{0.34}In_2S_{2.46}$
	In	56.07	
	S	19.27	
ZIS-7h	Zn	14.13	$Zn_{1.01}In_2S_{4.36}$
	In	48.92	
	S	29.79	

Table S4. The element atom contents measured by organic element analyzer (OEA)

Samples	S (wt.%)	theoretical value of S (wt.%)	normalization
ZIS-3.5h	21.06	30.26	$Zn_xIn_yS_{2.78}$

Table S5 Summary of the H_2O_2 yield rate of different photocatalysts

Photocatalysts	Light	Dosage ($g\ L^{-1}$)	Reaction solution	H_2O_2 yield rate ($\mu M\ h^{-1}$)	Ref.
$g\text{-}C_3N_4$	300 W Xe lamp $\lambda > 420$ nm	1	Pure water	54.87	1
$In_2S_3@O_v$ / In_2O_3	300 W Xe lamp $\lambda > 420$ nm	0.75	Pure water	206.45	2
Au / $BiVO_4$	2000 W Xe lamp $\lambda > 420$ nm	1.67	Pure water	4.2	3
Polyimide / $ZnIn_2S_4$	300 W Xe lamp $\lambda>420$ nm	0.1	Pure water	~41.11	4
Ni_{SAPs}-PuCN	300 W Xe lamp $\lambda\geq420$ nm	1	Pure water	342.2	5
cyclodextrin-pyrimidine polymer	300 W Xe lamp $\lambda\geq420$ nm	0.25	Pure water	139.3	6
CTF-BDDBN	300 W Xe lamp $\lambda>420$ nm	0.6	Pure water	58.33	7
10 % - Ti_3C_2 / TiO_2	UV light (λ =365 nm)	1	Water / ethanol	179.7	8
Ag / $ZnFe_2O_4$-Ag-Ag_3PO_4 (111)	AM 1.5 G	1	Water / methanol	103.15	9
EG-ZIS ($ZnIn_2S_4$)	LED lamp (100 $mW\ cm^{-2}$)	0.4	Water / isopropanol	229.13	10
$ZnIn_2S_4$ with dual vacancies	**300 W Xe lamp $\lambda\geq420$ nm**	**0.5**	**Pure water**	**199.30**	**This work**

Table S6. Summary of average electron lifetime deduced from the TRPL spectra

Samples	τ_1 (ns)	τ_2 (ns)	A_1	A_2	Average lifetime $<\tau>$ (ns)	χ^2
ZIS-3.5h	5.08	56.73	9640.18	1086.38	33.86	0.99
ZIS-7h	6.03	60.16	9276.41	1247.71	37.04	0.99

The average lifetime is calculated by equation:

$$< \tau >= \frac{A_1\tau_1^2 + A_2\tau_2^2}{A_1\tau_1 + A_2\tau_2}$$

χ^2: the goodness of fit parameter.

References

1. S. Gou, C. Wang, Z. Gong, Q. Wang, X. Li, X. Chen, J. Wang, J. Ma and Y. Zhu, Three-dimensional charge carrier transport channel enhanced photocatalytic H_2O_2 production in pure water over g-C_3N_4, *Sep. Purif. Technol.*, 2025, **354**, 128829.
2. X. Chen, W. Zhang, L. Zhang, L. Feng, C. Zhang, J. Jiang and H. Wang, Construction of Porous Tubular In_2S_3@In_2O_3 with Plasma Treatment-Derived Oxygen Vacancies for Efficient Photocatalytic H_2O_2 Production in Pure Water Via Two-Electron Reduction, *ACS Appl. Mater. Interfaces*, 2021, **13**, 25868-25878.
3. H. Hirakawa, S. Shiota, Y. Shiraishi, H. Sakamoto, S. Ichikawa and T. Hirai, Au Nanoparticles Supported on $BiVO_4$: Effective Inorganic Photocatalysts for H_2O_2 Production from Water and O_2 under Visible Light, *ACS Catal.*, 2016, **6**, 4976-4982.
4. X. Liu, X. Dong, Y. Wang, J. Gao, N. Zheng and X. Zhang, Polyimide/$ZnIn_2S_4$ heterostructures toward outstanding photocatalytic H_2O_2 production from pure water and air, *Appl. Surf. Sci.*, 2024, **643**, 158637.
5. X. Zhang, H. Su, P. Cui, Y. Cao, Z. Teng, Q. Zhang, Y. Wang, Y. Feng, R. Feng, J. Hou, X. Zhou, P. Ma, H. Hu, K. Wang, C. Wang, L. Gan, Y. Zhao, Q. Liu, T. Zhang and K. Zheng, Developing Ni single-atom sites in carbon nitride for efficient

photocatalytic H_2O_2 production, *Nat. Commun.*, 2023, **14**, 7115.

6. C. Chu, Q. Li, W. Miao, H. Qin, X. Liu, D. Yao and S. Mao, Photocatalytic H_2O_2 production driven by cyclodextrin-pyrimidine polymer in a wide pH range without electron donor or oxygen aeration, *Appl. Catal. B: Environ.*, 2022, **314**, 121485.
7. L. Chen, L. Wang, Y. Wan, Y. Zhang, Z. Qi, X. Wu and H. Xu, Acetylene and diacetylene functionalized covalent triazine frameworks as metal-free photocatalysts for hydrogen peroxide production: a new two-electron water oxidation pathway, *Adv. Mater.*, 2020, **32**, 1904433.
8. Y. Chen, W. Gu, L. Tan, Z. Ao, T. An and S. Wang, Photocatalytic H_2O_2 production using Ti_3C_2 MXene as a non-noble metal cocatalyst, *Appl. Catal. A: Gen.*, 2021, **618**, 118127.
9. X. Ma and H. Cheng, Facet-dependent photocatalytic H_2O_2 production of single phase Ag_3PO_4 and Z-scheme $Ag/ZnFe_2O_4$-Ag-Ag_3PO_4 composites, *Chem. Eng. J.*, 2022, **429**, 132373.
10. C. Ouyang, X. Quan, Z. A. Chen, K. Wang, X. Gu, Z. Hong and M. Zhi, Intercalation-and vacancy-enhanced internal electric fields in $ZnIn_2S_4$ for highly efficient photocatalytic H_2O_2 production, *J. Phys. Chem. C*, 2023, **127**, 20683-20699.